Evaluation of the agreement between Ultrasound-based and bi-planar X-Ray radiography-based assessment of the geometrical features of the Ischial Tuberosity in the context of the prevention of seating-related pressure injury

A.Berriot[1], N. Fougeron[1], X..Bonnet[1], H. Pillet[1] and P.Y. Rohan[1*]

[1]Institut de Biomécanique Humaine Georges Charpark, Arts et Metiers Institute Of Technology, 151 bvd de l'Hôpital, 75013. Paris, France

Abstract

The proper management of the local mechanical environment within soft tissues is a key challenge central the prevention of Pressure Ulcers (PUs). Magnetic Resonance (MR) imaging is the preferred imaging modality to measure geometrical features associated with PUs. It is a very time-consuming method and it represents a major barrier to the clinical translation of risk assessment tools. There is a growing enthusiasm of the community for the use of B-mode ultrasound imaging as a practical, alternative technology suitable for bedside or outpatient clinic use. The objective was to evaluate the agreement between US-derived measurements and bi-planar X-ray radiography-derived measurements of geometrical features of the Ischial Tuberosity in a realistic loaded sitting position in healthy volunteers. The reproducibility of the US-based assessment of radii of curvature, evaluated in a subset of 4 subjects using the IS0 5725-2 framework was 1.7 mm and 1.3 mm in the in the frontal and sagittal plane respectively (95 % CI = 3.5 mm and = 2.6 mm respectively). Out of the 13 subjects included, the ischial tuberosity border was visible on the US image of 7 healthy subjects only. The mean of differences computed on the 7 subjects using Bland-Altman plots were +3.3 mm and -5.7 mm in the frontal and sagittal planes respectively. The corresponding 95% CI in the frontal and sagittal planes were respectively 1.8 mm and 3.7 mm. These differences however were not statistically significant (Wilcoxon signed-rank test). More effort is needed to establish and standardise optimal measurement procedures and test protocols for the assessment of geometrical features of the IT using US.

1 INTRODUCTION

A Pressure Ulcer (PU) is defined as "*a localized injury to the skin and underlying soft tissue, usually over a bony prominence, caused by sustained pressure, shear or a combination of these*" (NPUAP, EPUAP, PPPIA, 2014). It is a complication primarily related to the care and treatment of individuals who have difficulty moving or changing positions: for example, those people with a disability and the elderly (Demarré et al., 2015). It appears in situations where excessive mechanical loads are applied to the skin, such as, for example, during mechanical interaction between a person and support surfaces (hospital bed) or medical devices (Manual Wheelchair, prosthetic socket, exoskeleton, etc.). PU prevention remains a major health challenge for Europe due to the human and financial cost of prolonged hospitalization, reduced quality of life, loss of autonomy and social isolation. However, current risk assessment tools do not allow for a correct identification of the risks nor putting an effective prevention in place (Coleman et al., 2013).

In the literature, a lot of research has sought to explain soft tissue injury risk factors in terms of the local mechanical environment (i.e. internal stresses and strains that satisfy mechanical equilibrium) within soft tissue (Oomens et al., 2015). In particular, it has been shown by combining an animal model of Deep Tissue Injury with computational modeling that direct deformation damage was only apparent when a certain strain threshold was exceeded (Ceelen et al., 2008). In humans, computational modelling of load-bearing soft tissue has shown that bony prominences induce substantial stress concentrations, which explains why these areas are vulnerable to pressure ulcers (Linder-Ganz et al., 2008). Laboratory and animal studies propose several aetiological mechanisms by which stress and internal strain interact with damage thresholds to result in pressure ulcer development including localized ischaemia (Loerakker et al., 2011), reperfusion injury (Jiang et al., 2011), impaired lymphatic drainage (Gray et al., 2016). and sustained cell deformation (Bouten et al., 2003; Gefen et al., 2008)

Based on the rationale that elucidating the relationship between external loads and internal local stresses and strains within loaded soft tissues has the potential of improving the management and prevention of PUs, several Finite Element (FE) models of the buttock have been proposed in the literature based on MRI or CT scan data (Al-Dirini et al., 2016; Levy et al., 2013; Linder-Ganz et al., 2007; Luboz et al., 2018; Zeevi et al., 2017). Because of the limited availability of MRI or CT-Scan systems and of the long segmentation time associated with the creation of full 3D subject specific FE models from these imaging systems, all the studies in the literature included the data of only one individual (Al-Dirini et al., 2016; Luboz et al., 2014). As far as the authors are aware of, the only attempts to account for this variability were limited to (i) semi-3D modelling (N=6 able-bodied volunteers in (Linder-Ganz et al., 2007); N=12 in (Linder-Ganz et al., 2008); and N=6 in (Linder-Ganz et al., 2009)) and (ii) one attempt at 3D modelling (N=6 in (Moerman et al., 2017)). In addition, the representation of a realistic unloaded sitting position is jeopardized by the experimental limitations of MRIs and CT-scans: Long acquisition times of MR imaging prevent a prolonged unloaded sitting configuration without resorting to devices (Al-Dirini et al., 2016) while the confinement of the scanner limits the acquisition to the lying position only (Luboz et al., 2014).

Recent developments in 3D reconstruction techniques from low dose calibrated bi-planar X-ray imaging (EOS imaging, Paris, France) provide a promising alternative tool for patient-specific validated 3D modelling of the pelvis (Ghostine et al., 2017). Moreover, unlike CT scanner or MRI systems where the patient is in a supine position, this technique provide bi-planar images of the subject in a weight-bearing position.

In a previous study, and as an alternative to MRI-based/CT-scan-based assessment, a methodology combining low-dose biplanar X-ray images (EOS imaging, Paris, France), B-mode ultrasound images and optical scanner acquisitions in a non-weight-bearing sitting posture has been proposed for the fast generation of patient-specific FE models of the buttock and applied to 6 healthy subjects (Macron et al., 2018).To investigate the ability of a local model of the region beneath the ischium to capture the internal response of the buttock soft tissues predicted by a complete 3D FE model from a limited number of parameters, a simplified model was developed based on data compatible with daily clinical routine (Macron et al., 2020). This study highlighted that the local mechanical environment within soft tissues is very sensitive (in the statistical sense i.e. variance-based sensitivity analysis) to the geometry of bony prominences and the relative thickness of the different soft tissue elements. Of particular interest, the sensitivity analysis showed that the maximum shear strain in the muscle tissue was very sensitive (29%) to the radius of curvature of the ischium in the plane perpendicular to the shortest radius of curvature. These results are in line with other results in the literature supporting the widely accepted idea that bone geometry will affect internal stresses and strains occurring under bony prominences (see for example (Gefen, 2010; Luboz et al., 2015) for heel ulcers).

B-mode ultrasound (US) imaging represents a promising alternative for assessing geometrical feature-related risk factor bedside or in a clinic with standard medical equipment. US imaging offers the advantages of being portable, non-invasive, with few contraindications and rapid result interpretation. There is therefore a high interest in the community for developing clinical protocols that are suited to reliable parameter assessment (Akins et al., 2016; Gabison et al., 2019; Swaine et al., 2018). If the measurement of the adipose and muscle tissue thicknesses in the vicinity of the ischium using US has been shown to be both reliable and highly correlated with MRI assessment (Akins et al., 2016), the measurement of the radius of curvature of the ischium, was, on the contrary, reported to have a poor inter operator reliability (Akins et al., 2016; Swaine et al., 2018).

In this perspective, we propose to evaluate, in this exploratory study, the agreement between US-derived and bi-planar X-ray radiography-derived measurements of geometrical features of the Ischial Tuberosity (IT) in a realistic loaded sitting position in healthy volunteers, to quantify the global standard deviation of reproducibility using the ISO standard 2725-2 and to quantify the influence of the angular position of the pelvis in the seated position on the US-based assessment of radii of curvature

2 METHODS

For the sake of clarity, only the experimental material previously acquired in the studies of (Macron et al., 2020, 2018) and pertaining to the current study are briefly recalled hereunder in Section 2.1.

2.1 Participants and protocol

Data of 13 healthy subjects (8 men and 5 women; age: 26 ± 5 years, weight: 70 ± 9 kg, BMI: 22.6 ± 3.4 kg/m2) previously acquired in the studies of (Macron et al., 2020, 2018) were used.

Biplanar radiographs were taken in frontal and sagittal views using the EOS low-dose imaging device (EOS imaging, Paris, France). The US acquisition of the sub-dermal tissue in the region beneath the IT was performed using a commercial device (Aixplorer, SuperSonic Imagine, France) with a linear US probe of 8 MHz central frequency (SuperLinear SL 15-4). A custom-made stool specifically designed for the experiment allowed to fix the US probe at the level of the seat inside the EOS cabin (figure 1(a)). A cross-shaped notch was made in the seat to fix the US probe in two orthogonal positions.

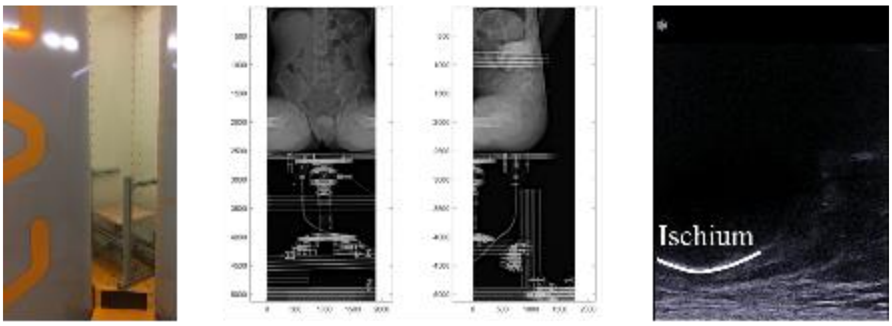

(a) (b) (c)

Figure 1: (a) Custom-made stool allowing to fix the US probe at the level of the seat inside the EOS cabin (b) bi-planar X-ray radiographies acquired in the loaded sitting position (c) US image in sitting loaded configuration with indication of ischium contour

The subject was asked to sit on the stool in the EOS cabin and, with the help of the on-screen display of the US device, was instructed to self-adjust the position of his/her ischium with the center of the screen. Two sets of data were then acquired with the subject in the loaded sitting position: the first one with the US probe in the frontal plane and the second one with the US probe in the sagittal plane. For each acquisition, a pair of bi-planar X-rays (EOS imaging, Paris, France) were acquired (with a pixel size of 0.179×0.179 mm) (figure 1(b)) immediately followed by a US video clip (pixel size of 0.085×0.085 mm), during which the subject was asked to slowly unload his weight with his arms while visually keeping the ischium as aligned as possible with the probe (figure 1(b-c)). This allowed to measure soft tissue thickness in the unloaded position. An additional pair of radiographs was also acquired in the standardized free standing position (Faro et al., 2004) for the purpose of 3D reconstruction of the pelvis from the EOS radiographs according to the procedure developed previously by (Mitton et al., 2006)

2.2 Data Analysis

2.2.1 Bimodal image registration

3D reconstruction of the pelvis (figure 2(a)) was performed from the EOS radiographs in the standing position according to the procedure developed previously by (Mitton et al., 2006). The 3D subject-specific model of the pelvis was then projected on the frontal and sagittal radiographs in the loaded sitting positions (in both the acquisition with the US probe in the frontal plane and the acquisition with the US probe in the sagittal plane). The position of the pelvis was manually adjusted until the contours matched those of the radiographs (figure 2(c)). The pelvic coordinate system (figure 2(a)) was defined from the left and right acetabula and S1 endplate of the 3D reconstruction following the definition given by (Dubois, 2014).

Similarly, the 3D CAD model of the linear US probe (figure 2(b)) was projected on the frontal and sagittal radiographs in the loaded sitting positions. The position was manually adjusted until the contours matched those of the radiographs (figure 2(c)). The probe coordinate system (figure 2(b)) was defined from the corners of the top part of the probe (transducer array). The 2D US image was positioned in the 3D EOS cabin space using the probe coordinate system (figure 2(d)).

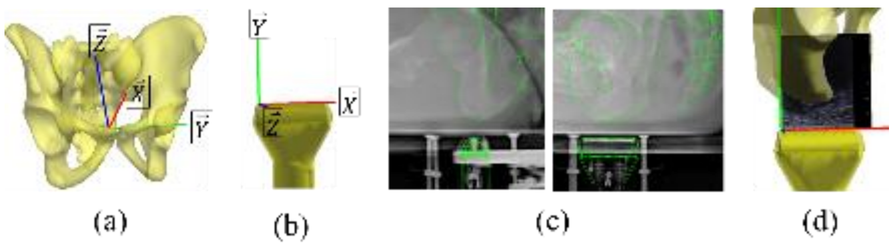

Figure 2: (a) 3D reconstruction of the pelvis and associated coordinate system (b) 3D CAD model of the linear US probe and associated coordinate system (c) cropped frontal and sagittal radiographs in the loaded sitting position with projection of i) 3D reconstruction of the pelvis and ii) 3D CAD model of the probe respectively iv) Bimodal image registration

2.2.2 Assessment of morphological parameter

US-based assessment of radii of curvature (US-RoC) and soft tissue thickness (US-STT). In both acquisitions (US probe in the frontal and sagittal planes respectively), 10 points were manually selected on the lowest part of the ischial tuberosity border visible on the US image in the seated position (figure 3(a)). The radius of curvature (figure 3(b)) was computed using a least-squares regression procedure using a custom-made MATLAB subroutine (MathWorks, Natick, MA, USA). The height of the selection, denoted Δz, was defined as the difference between maximum-altitude and the minimum-altitude points (figure 3(a)). The vertical component of the distance between lowest point of the IT and overlying skin surface was used to define the soft tissue thickness.

EOS-based assessment of the radii of curvature (EOS-RoC) and soft tissue thickness (EOS-STT). In both acquisitions (US probe in the frontal and sagittal planes respectively), the pelvis surface mesh intersecting points with the US probe plane were computed using a custom-made MATLAB subroutine (MathWorks, Natick, MA, USA). The points in the range Δz (previously determined for each configuration and for each subject) from the minimum-altitude point were selected. The radius of curvature was computed using the same least-squares regression procedure as for the US-based data points. Both the US-based and EOS-based least squares fitting circles were superposed on US image and 3D reconstruction of pelvis in the EOS cabin (global) coordinate system (figure 3(c)). The vertical component of the distance between the lowest point of the pelvis surface mesh intersecting with the US probe plane and overlying skin surface was used to define the soft tissue thickness.

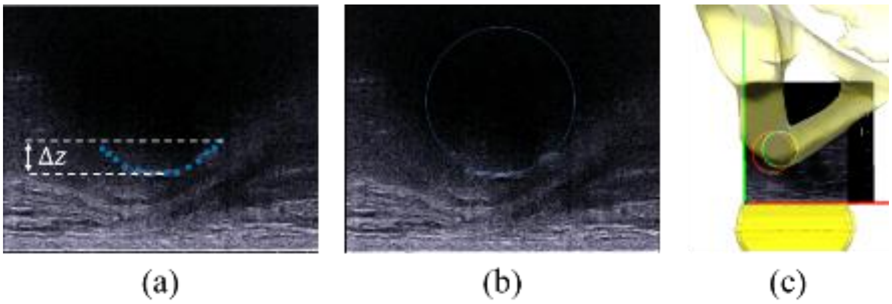

Figure 3: (a) Points manually selected on the inferior border of each IT (b) least squares fitting circle (c) US-based and EOS-based least squares fitting circles (respectively in red and green) superposed on US image and 3D reconstruction of pelvis in the EOS cabin (global coordinate system).

2.2.3 Statistical analysis

On a subset of 4 subjects (26 ± 1 year old), the inter-observer reproducibility standard deviation (SD_r) of the US-based assessment of radii of curvature was computed using the method described in the ISO standard 5725 (ISO, 1994). Each US image was processed 3 times by 3 operators in both acquisitions (US probe in the frontal and sagittal planes respectively). Reproducibility was estimated by computing the 95% confidence interval (95%CI) ($=2\cdot SD_r$).

The agreement between the US-based and EOS-based assessment of radii of curvature of the IT was described graphically with a Bland-Altman plot with mean of differences, reported with corresponding 95% confidence interval (CI), and lower and upper limits of agreement, calculated as mean ± 1.96 x standard deviation. Differences were assessed using a Wilcoxon-Signed-Rank Test (paired data) at the default 5 % significance level and was further described

2.2.4 Impact of pelvis angular position on the computed radii of curvature

A sensitivity study was performed to quantify the influence of the angular position of the pelvis in the seated position on the US-based assessment of radii of curvature.

Prior to this step, the maximum difference in the relative angular position of each pelvis to that of the average pelvic pose (averaged position and orientation) was quantified as follows: For each acquisition, the angular position of the pelvis frame was expressed in the EOS cabin (global) coordinate system. The orientation matrix of the relative angular position of each pelvis to that of the average pelvic pose was calculated. The decomposition of the rotation matrix was done using the XYZ rotation sequences of Cardan angles. The averaged position and orientation of all the pelvic frames was computed.

The procedure for the sensitivity study was the following: Each pelvis was repositioned in the averaged pelvic position (i.e. transformed so that the pelvis frame is aligned with that of the average pelvic pose). Then, for each pelvis, the pelvic obliquity (rotation around the global X-axis) and the anterior/posterior tilt (rotation around the global Y-axis) were modified independently by an increment of 5°, 10° and 15°. For each configuration, the (EOS-based) radius of curvature was computed according to the procedure described in section 2.2.2.

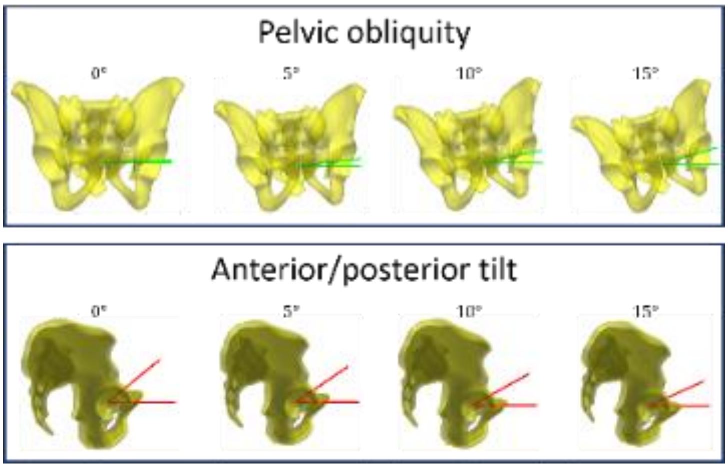

Figure 4: To assess the impact of small perturbations of the pelvic angular position during seating on the radius of curvature estimated using the procedure described in section 2.2.2, both (a) the pelvic obliquity and (b) the anterior/posterior tilt were modified independently by an increment of 5°, 10° and 15° and the radius of curvature was computed.

3 RESULTS

Out of the 13 subjects included, the ischial tuberosity border was visible on the US image of 7 healthy subjects only (4 men and 3 women; age: 28 ± 6 years, weight: 66 ± 7 kg, BMI: 21.6 ± 2.2 kg/m2). The results presented in this section therefore focuses on these 7 subjects only.

3.1 Assessment of morphological parameter

The reproducibility of the US-based assessment of radii of curvature was 1.7 mm (95% CI = 3.5 mm) in the frontal plane and 1.3 mm (95 % CI = 2.6 mm) in the sagittal plane respectively.

The results of the bimodal image registration and of the assessment of the radii of curvature and soft tissue thickness in both acquisitions (US probe in the frontal and sagittal planes respectively) are given in Table 1 below together with the results of the US-based and EOS-based assessment of Radii Of Curvature (RoC) and Soft Tissue Thickness (STT).

Table 1: Results of the bimodal image registration and of the assessment of the radii of curvature and soft tissue thickness in both acquisitions. US-based (red) and EOS-based (green) least squares fitting circles are superposed on US image and 3D reconstruction of pelvis in the EOS cabin (global coordinate system). All dimensions are in mm.

	Probe in the frontal plane (mm)			**Probe in the sagittal plane (mm)**		
1	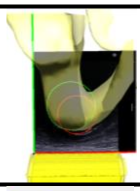	US-ROC	12.2	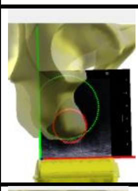	US-ROC	12.5
		EOS-RoC	15.4		EOS-RoC	23.9
		Difference	-3.2		Difference	-11.4
		US-STT	11.7		US-STT	12.2
		EOS-STT	14.4		EOS-STT	14.5
		Difference	-2.7		Difference	-2.3
2	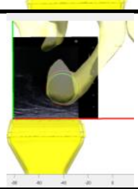	US-ROC	13.9	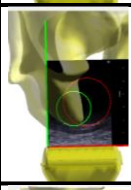	US-ROC	18.8
		EOS-RoC	12.3		EOS-RoC	13.6
		Difference	1.6		Difference	5.2
		US-STT	11.6		US-STT	16.1
		EOS-STT	11.5		EOS-STT	16.3
		Difference	0.1		Difference	-0.2:
3	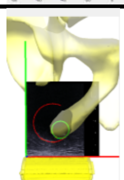	US-ROC	16.5	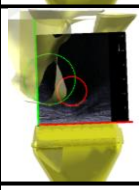	US-ROC	13.1
		EOS-RoC	7.4		EOS-RoC	11.7
		Difference	9.1		Difference	1.4
		US-STT	12.8		US-STT	12.6
		EOS-STT	14		EOS-STT	14.8
		Difference	-1.2		Difference	-2.2
4		US-ROC	20.4		US-ROC	8.5
		EOS-RoC	8.6		EOS-RoC	6.0
		Difference	11.8		Difference	-2.7
		US-STT	16.3		US-STT	10.2
		EOS-STT	12.6		EOS-STT	21.5

	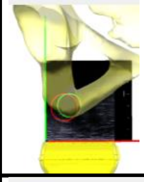	Difference	3.7	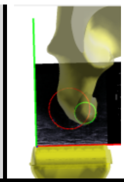	Difference	-11.3
5	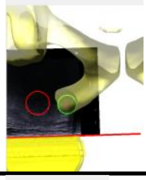	US-ROC EOS-RoC Difference US-STT EOS-STT Difference	8.6 6.8 1.8 15.7 16.6 -0.9	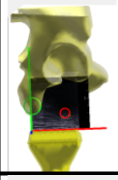	US-ROC EOS-RoC Difference US-STT EOS-STT Difference	7.2 9.9 -2.7 13.9 19.1 -5.2
6	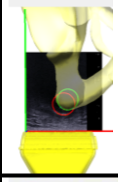	US-ROC EOS-RoC Difference US-STT EOS-STT Difference	9 8.4 0.6 13.3 16.3 -3	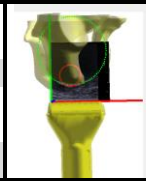	US-ROC EOS-RoC Difference US-STT EOS-STT Difference	11.4 36.8 -25.4 16.4 18.1 -1.7
7	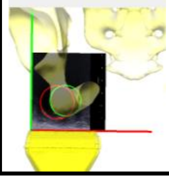	US-ROC EOS-RoC Difference US-STT EOS-STT Difference	14 12.7 1.3 8.8 11.7 -2.9	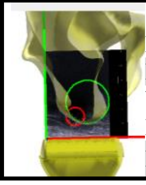	US-ROC EOS-RoC Difference US-STT EOS-STT Difference	6.9 16.2 -9.3 8.7 11.2 -2.5

Figure 5 below shows the Bland-Altman plot describing the agreement between US-based and EOS-based assessment of radii of curvature in the frontal and sagittal planes respectively. The bias or mean of differences were +3.3 mm and -5.7 mm in the frontal and sagittal planes respectively. The mean differences are not zero in either case and this means that, on average, the US measures 3.3 mm more than the EOS-based in the frontal plane (overestimation) and 5.7 less in the sagittal plane (underestimation) respectively. As can be further seen, the differences were of both positive and negative values. The corresponding 95% CI in the frontal and sagittal planes were respectively 1.8 mm and 3.7 mm. The lower and upper limits of agreement were respectively -6.2 mm and 12.8 mm in the frontal plane. The lower and upper limits of agreement were respectively -25 mm and 13.6 mm in the sagittal plane.

Results of the Wilcoxon signed-rank-test, however did not allow rejecting the null hypothesis about the differences between the US-based and EOS-based ROC (p values of 0.16 and 0.30 in the frontal and sagittal planes respectively). Determining soft tissue thickness in the unloaded position was not always possible because the IT was not systematically visible on the US images.

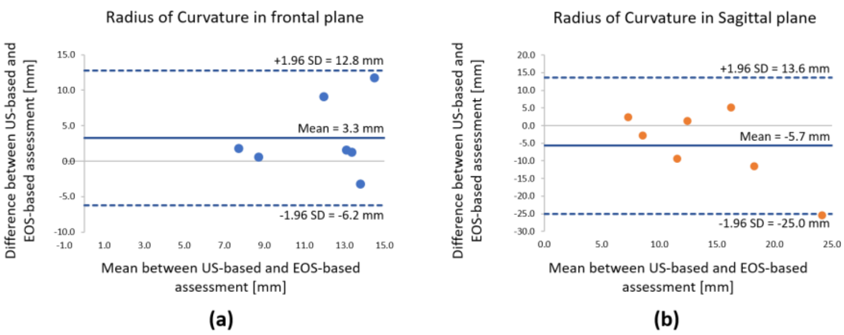

Figure 5 Plot of differences between US-based and EOS-based assessment of radii of curvature vs. the mean of the two measurements (data from table 1) in the frontal (a) and sagittal (b) planes respectively.

3.2 Impact of pelvis angular position on the computed radii of curvature

The maximum difference in the relative angular position of each pelvis to that of the average pelvic pose was 17° (anterior posterior tilt). This allows to estimate an order of magnitude of the inter-individual variability in pelvis pose in realistic loaded sitting position in healthy volunteers.

Increasing the pelvic obliquity, lead, on average, to a decrease in the EOS-based radius of curvature assessed (0.80 mm, 1.5 mm and 18 mm respectively for a rotation of 5°, 10° and 15° in the frontal plane; 0.2 mm, 0.6 mm and 0.1 mm respectively in the sagittal plane for a rotation of 5°, 10° and 15°).

Increasing the anterior/posterior tilt, on average lead to a relatively small increase in the EOS-based radius of curvature assessed (0.80 mm, 1.4 mm and 2.5 mm respectively for a rotation of 5°, 10° and 15° respectively in the frontal plane; 1.4 mm, 1.7 mm and 2.7 mm respectively in the sagittal plane for the 3 rotations).

4 DISCUSSION

The objective of this exploratory study was to evaluate the agreement between Ultrasound-based and bi-planar X-Ray radiography-based assessment of the geometrical features of the Ischial Tuberosity in the context of the prevention of seating-related pressure injury. Assessment of the geometry of bony prominences is important for PU prevention because the local mechanical environment within soft tissues – which has been shown to be a correlated to soft tissue injury risk (Ceelen et al., 2008; Loerakker et al., 2011) - is very sensitive (in the statistical sense i.e. variance-based sensitivity analysis) to the geometry of bony prominences (Gefen, 2010; Luboz et al., 2015; Macron et al., 2020). Based on these results, establishing routine ultrasound scans of the ischium could potentially lead to development of new ultrasound-based risk assessment tools that are more specific for identifying susceptibility to seating-related pressure injuries, particularly considering the individual's internal anatomy. This probably explains the increasing enthusiasm of the community for the measurement of this geometrical feature-related risk factor using medical imaging.

Results obtained in this contribution on N=7 healthy however suggest that more effort is needed to establish and standardise optimal measurement and processing procedures and test protocols for the assessment of geometrical features of the IT using US. On average, US-based assessment of radius of curvature underestimated that of the EOS-based in the frontal plane and overestimated in the sagittal plane respectively. This may be partly due to the fact that approximating the ischial tuberosity by a torus (two radii of curvature in the frontal and sagittal planes which are not necessarily aligned with the IT orientation) is too gross and leads to biases in the assessment of morphological parameters. This can also be explained by the ultrasound imaging artefacts inherent to this technology, which, make the detection of bone contours less robust. The fitting of the circle is also dependent on the pelvic posture in sitting. If participants are sitting forward or backward, the circumference of the lowest point of the IT changes dramatically and it is very difficult to measure since the IT is flattened.

In the literature, Swaine and colleagues (2008) represented the ischium using two radii of curvature (along anatomical planes, representing the shortest and longest axis) – other authors limiting the analysis to only one plane (Akins et al., 2016). If a good inter-rater reliability for soft tissue thickness assessment of the soft tissue layers overlying inferior curve of IT (skin & fat, tendon & muscle, while thickness) are generally reported, (Swaine et al., 2018) observed a poor inter-rater reliability of sonographers in measuring diameter of the inferior curve of IT. This result is in contrast to that reported by (Akins et al., 2016) who reported an higher concordance value (ICC = 0.712). However, this earlier study utilised a single scan operator to acquire images and two operators to post-process the data on the same images. Such a post processing protocol will inevitably impact the decisions an operator must make during real-time image acquisition and measurement. In this study, a custom-made stool was designed to eliminate the uncertainty related to exclude the impact of inter-operator variability in transducer rotation, medial/lateral and cranial/caudal tiling and pressure exerted over the tissues during examinations. Yet, the reproducibility of the US-based assessment of radii of curvature were relatively high (95% CI = 3.5 mm in the frontal plane and 95 % CI = 2.6 mm in the sagittal plane respectively), highlighting the effect of the procedure for extracting morphologic parameters.

The results obtained in our study for US-based assessment of radius of curvature are 13.5±4.1 mm (range [8.6 mm – 20.4 mm]) in the frontal plane and 11.2±4.2 mm (range [6.9 mm – 18.8 mm]) in sagittal plane respectively. This is within the same range as reported by (Akins et al. 2016) (between 8.5 mm and 20.0 mm) and (Swaine et al. 2018) (24.2±5 mm in the short axis, 30.0±8 mm in the long axis, respectively. Out of the 13 subjects included in the studies of (Macron et al., 2020, 2018), 6 were excluded for the assessment of the IT curvature in this study since the ischium was not visible due to thick tissue layer of subjects. This can emphasize US-based measurement of IT curvature is highly dependent not only on operator but also the subject. The use of a linear probe represents a limitation of the current study since it is not adapted it has limited penetration. As a perspective work, the use of a curvilinear ultrasound probe will be explored to allow for imaging patients where the image depth penetration and width capture requirements are greater, such as young trauma patients with high muscle bulk, morbidly obese patients with significant subcutaneous fat and patients with fluid overload.

The results obtained in this study for EOS-based assessment of radius of curvature are 10.2±3.2 mm (range [6.8 mm – 15.4 mm]) in the frontal plane and 16.9±10.4 mm (range [6.0 mm – 36.8 mm]) in sagittal plane respectively. A plausible explanation for the discrepancy between US-based and EOS-based assessment of radii of curvature is the level of accuracy if 3D-reconstructions from bi-planar X-ray images comparaed to CT-scan data. It has been reported that shape differences between 3D models obtained from bi-planar X-rays and CT-scan are, on average 1.6 mm (Mitton et al., 2006).

Recent studies suggest that B-mode Ultrasound imaging constitutes a promising alternative that could overcome some limitations of MRI. Further investigations need to be done in order to estimate the system’s overall accuracy in a controlled laboratory setting using precisely built phantom. To make a conclusion on the potential clinical accuracy, the differences between the clinical and laboratory settings must be carefully examined.

References

Akins, J.S., Vallely, J.J., Karg, P.E., Kopplin, K., Gefen, A., Poojary-Mazzotta, P., Brienza, D.M., 2016. Feasibility of freehand ultrasound to measure anatomical features associated with deep tissue injury risk. Med. Eng. Phys. 38, 839–844. https://doi.org/10.1016/j.medengphy.2016.04.026

Al-Dirini, R.M.A., Reed, M.P., Hu, J., Thewlis, D., 2016. Development and Validation of a High Anatomical Fidelity FE Model for the Buttock and Thigh of a Seated Individual. Ann. Biomed. Eng. 44, 2805–2816. https://doi.org/10.1007/s10439-016-1560-3

Bouten, C. V., Oomens, C.W., Baaijens, F.P., Bader, D.L., 2003. The etiology of pressure ulcers: skin deep or muscle bound? Arch. Phys. Med. Rehabil. 84, 616–619. https://doi.org/10.1053/apmr.2003.50038

Ceelen, K.K., Stekelenburg, A., Loerakker, S., Strijkers, G.J., Bader, D.L., Nicolay, K., Baaijens, F.P.T., Oomens, C.W.J., 2008. Compression-induced damage and internal tissue strains are related. J. Biomech. 41, 3399–3404. https://doi.org/10.1016/j.jbiomech.2008.09.016

Coleman, S., Gorecki, C., Nelson, E.A., Closs, S.J., Defloor, T., Halfens, R., Farrin, A., Brown, J., Schoonhoven, L., Nixon, J., 2013. Patient risk factors for pressure ulcer development: Systematic review. Int. J. Nurs. Stud. 50, 974–1003. https://doi.org/10.1016/j.ijnurstu.2012.11.019

Demarré, L., Van Lancker, A., Van Hecke, A., Verhaeghe, S., Grypdonck, M., Lemey, J., Annemans, L., Beeckman, D., 2015. The cost of prevention and treatment of pressure ulcers: A systematic review. Int. J. Nurs. Stud. 52, 1754–1774. https://doi.org/10.1016/j.ijnurstu.2015.06.006

Dubois, G., 2014. Contribution à la modélisation musculo-squelettique personnalisée du membre inférieur combinant stéréoradiographie et ultrason. (phdthesis). Ecole nationale supérieure d'arts et métiers - ENSAM.

Faro, F.D., Marks, M.C., Pawelek, J., Newton, P.O., 2004. Evaluation of a functional position for lateral radiograph acquisition in adolescent idiopathic scoliosis. Spine 29, 2284–2289.

Gabison, S., Hayes, K., Campbell, K.E., Swaine, J.M., Craven, B.C., 2019. Ultrasound imaging of tissue overlying the ischial tuberosity: Does patient position matter? J. Tissue Viability. https://doi.org/10.1016/j.jtv.2019.07.001

Gefen, A., 2010. The biomechanics of heel ulcers. J. Tissue Viability 19, 124–131. https://doi.org/10.1016/j.jtv.2010.06.003

Gefen, A., van Nierop, B., Bader, D.L., Oomens, C.W., 2008. Strain-time cell-death threshold for skeletal muscle in a tissue-engineered model system for deep tissue injury. J. Biomech. 41, 2003–2012. https://doi.org/10.1016/j.jbiomech.2008.03.039

Ghostine, B., Sauret, C., Assi, A., Bakouny, Z., Khalil, N., Skalli, W., Ghanem, I., 2017. Influence of patient axial malpositioning on the trueness and precision of pelvic parameters obtained from 3D reconstructions based on biplanar radiographs. Eur. Radiol. 27, 1295–1302. https://doi.org/10.1007/s00330-016-4452-x

Gray, R.J., Voegeli, D., Bader, D.L., 2016. Features of lymphatic dysfunction in compressed skin tissues – Implications in pressure ulcer aetiology. J. Tissue Viability 25, 26–31. https://doi.org/10.1016/j.jtv.2015.12.005

ISO, 1994, ISO 5725-2 Accuracy (Trueness and Precision) of Measurements Methods and Results.—Part 2: Basic Method for the Determination of Repeatability and Reproducibility of a Standard Measurement Method, International Organisation for Standardisation, Geneva, Switzerland (1994), Retrieved from https://www.iso.org/standard/69419.html

Jiang, L., Tu, Q., Wang, Y., Zhang, E., 2011. Ischemia-reperfusion injury-induced histological changes affecting early stage pressure ulcer development in a rat model. Ostomy. Wound Manage. 57, 55–60.

Levy, A., Kopplin, K., Gefen, A., 2013. Simulations of skin and subcutaneous tissue loading in the buttocks while regaining weight-bearing after a push-up in wheelchair users. J. Mech. Behav. Biomed. Mater. 28, 436–447. https://doi.org/10.1016/j.jmbbm.2013.04.015

Linder-Ganz, E., Shabshin, N., Itzchak, Y., Gefen, A., 2007. Assessment of mechanical conditions in sub-dermal tissues during sitting: a combined experimental-MRI and finite element approach. J. Biomech. 40, 1443–1454. https://doi.org/10.1016/j.jbiomech.2006.06.020

Linder-Ganz, E., Shabshin, N., Itzchak, Y., Yizhar, Z., Siev-Ner, I., Gefen, A., 2008. Strains and stresses in sub-dermal tissues of the buttocks are greater in paraplegics than in healthy during sitting. J. Biomech. 41, 567–580. https://doi.org/10.1016/j.jbiomech.2007.10.011

Linder-Ganz, E., Yarnitzky, G., Yizhar, Z., Siev-Ner, I., Gefen, A., 2009. Real-time finite element monitoring of sub-dermal tissue stresses in individuals with spinal cord injury: Toward prevention of pressure ulcers. Ann. Biomed. Eng. 37, 387–400. https://doi.org/10.1007/s10439-008-9607-8

Loerakker, S., Manders, E., Strijkers, G.J., Nicolay, K., Baaijens, F.P.T., Bader, D.L., Oomens, C.W.J., 2011. The effects of deformation, ischemia, and reperfusion on the development of muscle damage during prolonged loading. J. Appl. Physiol. 111, 1168–1177. https://doi.org/10.1152/japplphysiol.00389.2011

Luboz, V., Bailet, M., Boichon Grivot, C., Rochette, M., Diot, B., Bucki, M., Payan, Y., 2018. Personalized modeling for real-time pressure ulcer prevention in sitting posture. J. Tissue Viability 27, 54–58. https://doi.org/10.1016/j.jtv.2017.06.002

Luboz, V., Perrier, A., Bucki, M., Diot, B., Cannard, F., Vuillerme, N., Payan, Y., 2015. Influence of the Calcaneus Shape on the Risk of Posterior Heel Ulcer Using 3D Patient-Specific Biomechanical Modeling. Ann. Biomed. Eng. 43, 325–335. https://doi.org/10.1007/s10439-014-1182-6

Luboz, V., Petrizelli, M., Bucki, M., Diot, B., Vuillerme, N., Payan, Y., 2014. Biomechanical modeling to prevent ischial pressure ulcers. J. Biomech. 47, 2231–2236. https://doi.org/10.1016/j.jbiomech.2014.05.004

Macron, A., Pillet, H., Doridam, J., Rivals, I., Sadeghinia, M.J., Verney, A., Rohan, P.-Y., 2020. Is a simplified Finite Element model of the gluteus region able to capture the mechanical response of the internal soft tissues under compression? Clin. Biomech. 71, 92–100. https://doi.org/10.1016/j.clinbiomech.2019.10.005

Macron, A., Pillet, H., Doridam, J., Verney, A., Rohan, P.-Y., 2018. Development and evaluation of a new methodology for the fast generation of patient-specific Finite Element models of the buttock for sitting-acquired deep tissue injury prevention. J. Biomech. 79, 173–180. https://doi.org/10.1016/j.jbiomech.2018.08.001

Mitton, D., Deschênes, S., Laporte, S., Godbout, B., Bertrand, S., Guise, J.A. de, Skalli, W., 2006. 3D reconstruction of the pelvis from bi-planar radiography. Comput. Methods Biomech. Biomed. Engin. 9, 1–5. https://doi.org/10.1080/10255840500521786

Moerman, K.M., van Vijven, M., Solis, L.R., van Haaften, E.E., Loenen, A.C.Y., Mushahwar, V.K., Oomens, C.W.J., 2017. On the importance of 3D, geometrically accurate, and subject-specific finite element analysis for evaluation of in-vivo soft tissue loads. Comput. Methods Biomech. Biomed. Engin. 20, 483–491. https://doi.org/10.1080/10255842.2016.1250259

National Pressure Ulcer Advisory Panel, European Pressure Ulcer Advisory Panel, and Pan Pacific Pressure Injury Alliance, 2014, National Pressure Ulcer Advisory Panel, European Pressure Ulcer Advisory Panel, & Pan Pacific Pressure Injury Alliance Prevention and Treatment of Pressure Ulcers: Quick Reference Guide. Guidelines, Retrieved from http://www.npuap.org/wp-content/uploads/2014/08/Quick-Reference-Guide-DIGITAL-NPUAP-EPUAP-PPPIA-Jan2016.pdf (2014)

Oomens, C.W.J., Bader, D.L., Loerakker, S., Baaijens, F., 2015. Pressure Induced Deep Tissue Injury Explained. Ann. Biomed. Eng. 43, 297–305. https://doi.org/10.1007/s10439-014-1202-6

Swaine, J.M., Moe, A., Breidahl, W., Bader, D.L., Oomens, C.W.J., Lester, L., O'Loughlin, E., Santamaria, N., Stacey, M.C., 2018. Adaptation of a MR imaging protocol into a real-time clinical biometric ultrasound protocol for persons with spinal cord injury at risk for deep tissue injury: A reliability study. J. Tissue Viability, Seating Biomechanics 27, 32–41. https://doi.org/10.1016/j.jtv.2017.07.004

Zeevi, T., Levy, A., Brauner, N., Gefen, A., 2017. Effects of ambient conditions on the risk of pressure injuries in bedridden patients-multi-physics modelling of microclimate. Int. Wound J. https://doi.org/10.1111/iwj.12877